

DEVELOPMENT, CHARACTERIZATION, AND OPTIMIZATION OF PROCESS FOR MINIMAL  
FUNCTIONAL BARRIER AND CHANNEL WIDTH IN NITROCELLULOSE PAPER  
MICROFLUIDIC DIAGNOSTIC PLATFORMS

A Senior Project

Presented to

The Faculty of California State University,

San Luis Obispo

In Partial Fulfillment

of the Requirements for the Degree

Bachelor of Science

By

Ryan Daniel Silva

Advisor: Dr. David Clague

Date of Submission: September 2014

©2014

Ryan Daniel Silva

ALL RIGHTS RESERVED

# 1 Table of Contents

2	Introduction .....	8
2.1	Medical Diagnostics .....	8
2.1.1	Current Lab on a Chip Technology .....	10
2.2	Current paper-microfluidics technology .....	12
2.2.1	Microfluidic Platforms .....	12
2.2.2	Creating channels.....	14
2.3	Capability Gap to Be Addressed.....	18
2.3.1	Challenges to be addressed in this work.....	19
2.4	Summary of Intro .....	19
3	Materials .....	19
3.1	Papers.....	19
3.2	Lab Equipment .....	20
3.2.1	XEROX ColorQube 8570 .....	20
3.2.2	Food Coloring (FD&C Blue No. 1) .....	21
3.2.3	Lab Oven .....	22
3.2.4	Additional Equipment.....	22
3.3	Software .....	22
4	Methods and Results .....	23
4.1	Determining Optimal Baking Times and Temperatures .....	23
4.2	Determining Experimental Range .....	23
4.3	Process Characterization and Optimization .....	24
4.3.1	Wax Reflow Characterization.....	24
4.4	Practical Application – Minimal Feature Sizes .....	29
4.4.1	Determination of minimum functional barrier width .....	29
4.4.2	Determination of minimum functional channel width.....	33
4.4.3	Mock Devices .....	35
5	Conclusion .....	36
5.1	Optimal Process Parameters .....	36
5.2	Minimal Functional Feature Size.....	37
5.2.1	Functional Barrier Width .....	37
5.2.2	Functional Channel Width .....	37

5.2.3	Future Work .....	37
6	Works Cited .....	39

## LIST OF TABLES

Table 1: Millipore Corp's selection of Nitrocellulose Membrane .....	20
Table 2: Experimental Ranges for Time and Temperature .....	24
Table 3: Wax spreading as a function of Temperature, Time, and Membrane model. ....	27
Figure 4: Lateral Spreading, as a ratio of Desired Printed Width. n .....	28

## LIST OF FIGURES

Figure 1: Spaceflight Affect on Human Body. ....	9
Figure 2: Creating a Microfluidic Device in Paper. ....	12
Figure 3. 384-zone plate patterned in paper .....	13
Figure 4: Scanning Electron Microscope Image of Nitrocellulose. ....	14
Figure 5: Example of a device created by reshaping the platform. ....	16
Figure 6: Procedure for preparing a wax-based paper microfluidic device.....	17
Figure 7: Channel width in Paper. ....	18
Figure 8: Xerox 8570N .....	20
Figure 9: Loading Ink to XEROX 8570N. ....	21
Figure 10: Group of 0.5mm wide lines .....	25
Figure 11: Example of 0.5mm line cross-section. ....	26
Figure 12: Wax Flow over time .....	27
Figure 13: Devices to Test Minimal Functional Barrier Width. s. ....	30
Figure 14: Round Barrier Width Device Designs. ....	31
Figure 15: Round Barrier Width Devices and Results .....	32
Figure 16: Straight Line Barrier Width Devices and Results .....	32
Figure 17: Preliminary Channel Width Teting .....	33
Figure 18: Channel Width Testing Devices Results .....	34
Figure 19: Design of Mock Devices.....	35
Figure 20: Results of Mock Device Testing .....	36

## Abstract

A central goal of diagnostic microfluidics is to reduce the cost of diagnostic medicine by reducing the equipment and reagents needed to perform diagnostic tests. The literature has demonstrated that a wax printer can be used to pattern nitrocellulose paper with hydrophobic barriers to direct a sample in a defined reaction path, eliminating the need for external pumps and controllers. However, manufacturing methods for minimizing sample volume (and thus reagent volume) in a paper-diagnostic chip have not been well defined. In this work, we experimentally determine manufacturing processes for creating functional features of minimal size—effectively reducing the sample size and required reagents. We describe the methods for determining the effects that temperature, time, and substrate type have on printable feature size. Using this developed knowledge, we were able to create 400-micron barriers and demonstrate functional channels as narrow as 100 microns. By standardizing manufacturing methods, we have enabled future exploration of novel applications for wax-based paper-microfluidics.

## 2 Introduction

### 2.1 Medical Diagnostics

Modern medicine applies a large repertoire of diagnostic tests to direct the treatment of patients.

In order to properly treat a disease, a doctor must first be able to accurately diagnose it<sup>1</sup>

Diagnostics is necessary for identifying the presence and cause of disease, correctly assessing the nature of disease, designating an appropriate course of treatment, monitoring the effects of interventions, and determining drug resistance and/or the recurrence of existing disease.<sup>2</sup>

Modern diagnostic labs could not perform reliable and accurate tests without reliable power, refrigeration, and trained personnel. Unfortunately, one or more of these necessary resources may be lacking in poverty stricken areas such as Africa and in the final frontier –space.

Extended visits to space have a profound effect on the human body. The heart becomes smaller and weaker, body fluid decreases, muscles atrophy, and bones weaken. These effects are largely attributed to the microgravity environment experienced by an astronaut in space<sup>3</sup>. Figure 1 below shows altered body functions caused by space flight.



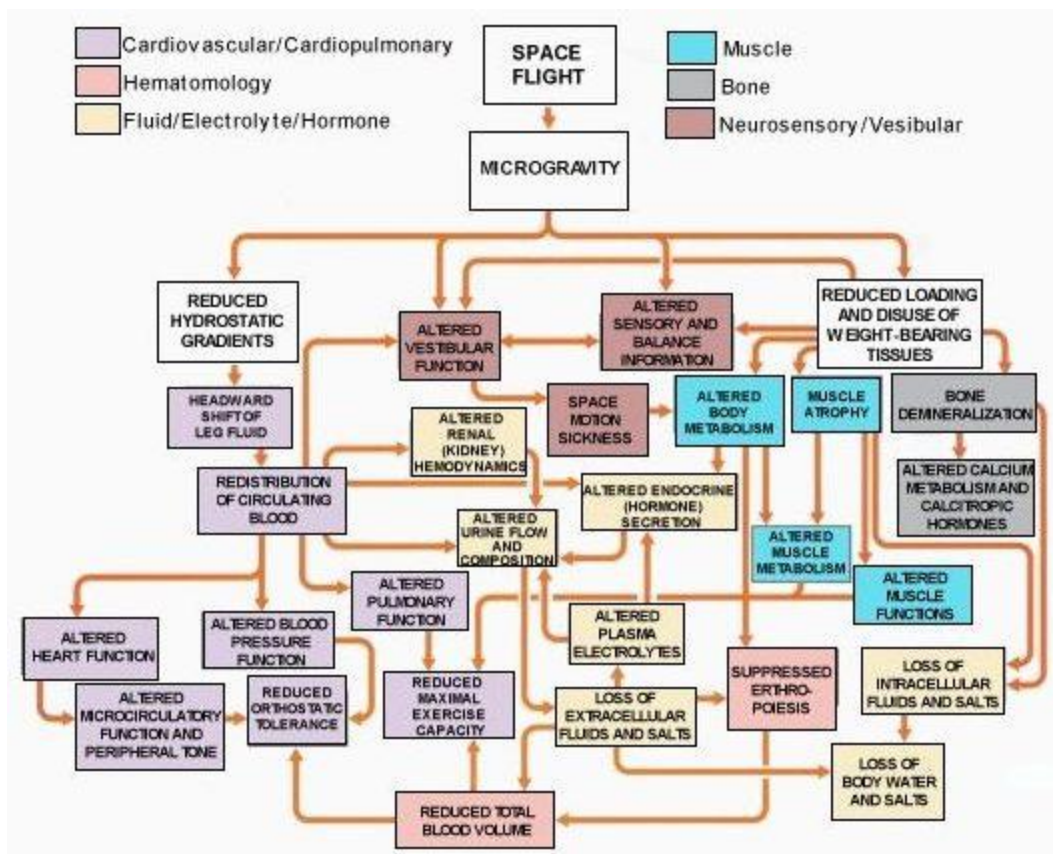


Figure 1: Spaceflight Effect on Human Body. This flowchart shows the many connections between spaceflight and human physiological responses<sup>3</sup>

One of the physiologic responses to extended space flight is the decrease in bodily fluids is caused by the upward shift of bodily fluids in space. Without gravity to draw fluid down to the legs, there tends to be an excess amount of fluid in the upper body. This causes astronauts to have puffy faces and ‘chicken legs’. The upward shift in fluid also causes an increase in pressure detected by the carotid baroreceptors. To return blood pressure to normal, the body will reduce body fluid volume by increasing urine production<sup>3</sup>. Physiologic status must be closely monitored to enable an intervention if an astronaut’s condition deviates from ‘space norm.’

Kidney function is quantified by glomerular filtration rate (GFR). GFR is how much filtrate is removed from the blood each minute. As kidneys fail, GFR will decrease. Directly

measuring GFR in space is difficult as it requires a blood collection and injection kit, a blood sample storage kit, a centrifuge, and a urine monitoring system.<sup>3</sup> Serum creatinine levels are much simpler to measure, and are closely related to GFR. As such, serum creatinine levels can be used to estimate GFR<sup>4</sup>. Measuring serum creatinine can only estimate GFR, but it is adequately sensitive and the possible ease-of-use benefits compared to a direct GFR measurement are great.

Serum creatinine levels can be measured relatively easily with the proper equipment; however, the size and weight restrictions of space flight severely reduce the availability of equipment. To outline the requirements of space diagnostic equipment, in June 2011, NASA released a whitepaper titled “Exploration Medical Capability Functional Requirements Document.” This paper outlines the medical capabilities required for a NASA space exploration mission. In the Laboratory Analysis section of the paper, NASA outlines the requirements for diagnostic hardware for long term (>30 days) missions. Devices on the shuttle “should minimize: mass, volume, consumables, reagents, and power.”<sup>5</sup> Lab on a chip technology is an attractive potential solution to these requirements.

### **2.1.1 Current Lab on a Chip Technology**

A new technology must be developed to reduce the resources needed to bring the monitoring and treatment benefits of modern medicine to resource-poor environments. The main focus of traditional microfluidics has been to create a “Lab on a Chip”. These glass or plastic devices combine multiple steps: preprocessing, reagent addition and signal detection, all onto a small chip the size of a microscope slide. The most sensitive of these devices can function using only picoliter sized aliquots of reagents and samples<sup>6</sup>. However, these systems require external

optics, pumps and detectors which deter their adoption in resource-poor environments<sup>6</sup>. Devices designed using a paper platform could eliminate the need for these complex exterior devices.

It is desirable to have a test that is sensitive at minimal sample volumes because usually many tests will have to be performed. Minimizing the sample volume required per test will allow more tests to be run without increasing patient sample donation, reducing negative impact on the patient. Using paper microfluidics, Martinez et al analyzed samples as small as 5  $\mu$ L for the presence of glucose and BSA simultaneously with great accuracy they were able to detect concentrations as low as 2.5mM of glucose and 0.38mM of BSA. The minimal detection ranges of clinically available dipsticks are 5mM for glucose and 0.75 $\mu$ M for protein<sup>7</sup>. Paper devices have not yet been demonstrated on as small a sample size or reagent size as traditional microfluidics. However, removing the need for excessive external equipment to perform a test makes paper extremely attractive for use in the field.

## 2.2 Current paper-microfluidics technology

Paper-microfluidics was established by George Whitesides at Harvard University. The initial designs were based on a chromatography paper platform due to its low-cost and its outstanding wicking abilities. As demonstrated in the Figure 2 hydrophobic barriers were created by soaking the paper in photoresist, creating a pattern with a light mask, and rinsing away the undeveloped photoresist.<sup>8</sup>

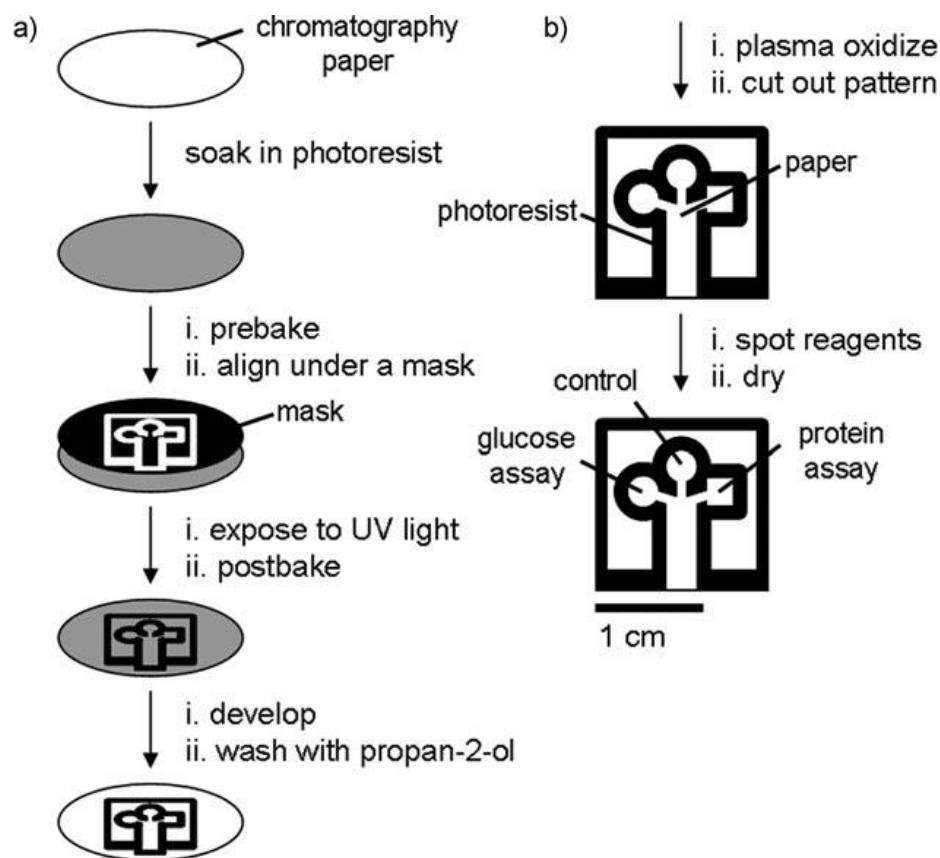


Figure 2: Creating a Microfluidic Device in Paper. This was the original schema for creating a paper microfluidic chip using chromatography and SU=8 photoresist<sup>7</sup>

### 2.2.1 Microfluidic Platforms

The different types of microfluidic designs are known as the platform. The platform is the main component of the chip and is the material through which sample flows. The platform provides a place to anchor detection regions, and deposit flow-directors. Platforms that consist of

cellulose or nitrocellulose are the most commonly called paper-microfluidic chips. Pictured below is a plate with 384 reaction zones patterned on cellulose paper.

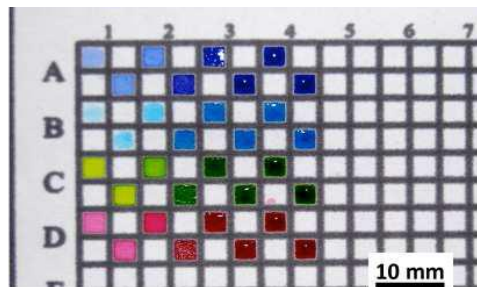


Figure 3: An example of a 384-zone plate patterned with wax in cellulose chromatography paper.<sup>9</sup>

#### 2.2.1.1 Nitrocellulose

Nitrocellulose, composed of cellulose nitrate, is an excellent substrate for protein binding because of strong charge-charge interactions and weak secondary forces.<sup>6</sup> Nitrocellulose is frequently used for protein immobilization and the procedures for doing so are well documented.<sup>6</sup> Nitrocellulose membrane also has a small, uniform pore size (as seen in the SEM image in Figure 4 below) which permits smooth and uniform sample distribution and barrier formation.<sup>6</sup> As such, it is a simple process to pattern devices on nitrocellulose membrane using a standard wax printer.

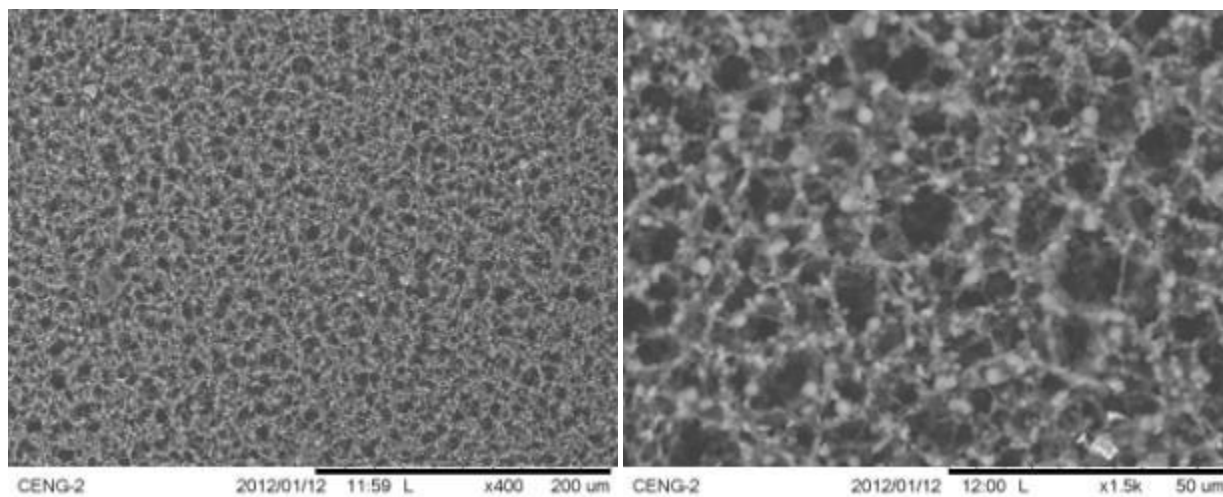


Figure 4: Environmental Scanning Electron Microscope Image of Nitrocellulose. At 400x (left) and 1500x (right) magnification.

These pictures demonstrate the relatively uniform and highly porous structure of nitrocellulose membrane

#### 2.2.1.2 *Cellulose*

Most published work in paper-microfluidics has been performed in cellulose paper. The advantages of cellulose paper are that it is a common, inexpensive, and safe. However, it is limited for use in diagnostics due to its poor ability to bind to proteins.<sup>10</sup>

### 2.2.2 *Creating channels*

Channels separate paper-microfluidic assays from traditional lateral flow assays (such as at-home pregnancy tests). Channels are the sections of the platform through which sample flows. Channel walls direct sample flow through reaction zones and to detection zones. These channels differentiate microfluidic devices from lateral flow assays which allow fluid to wick across the entire platform. Sample will flow throughout the entire width of channel it is in. By reducing the width of the channels, the amount of sample and reagent needed to perform a test is also reduced. Following is a summary of the current methods of creating channels.

#### 2.2.2.1 *Photoresist channels*

Chromatography paper was soaked in SU-8 2010 photoresist, covered with a printed mask, and exposed to UV light. The negative areas of the mask allowed UV light to pass through and polymerize the photoresist. The undeveloped photoresist was then removed using propan-2-ol. Then the paper was exposed to oxygen plasma to remove any residual undeveloped photoresist. Since photoresist is hydrophobic, it was used to form the walls of the channels, see Figure 2. The hydrophilic chromatography paper provided a hydrophilic capillary path for sample<sup>7</sup>.

#### 2.2.2.2 *Plasma-treated channels*

Whatman filter paper can be made hydrophobic with an AKD-heptane solution, making it impermeable to water. Patterns were mechanically cut into sheets of stainless steel to create a mask. The mask was placed above the substrate. When exposed to the plasma beam from a vacuum plasma reactor, the unmasked portions of the substrate were hit with the plasma, and thus made hydrophilic. Water was easily able to wick through the channels. Devices with built-in switches, filters, and separators were fabricated using these methods, and it was claimed that creating these features would be much more difficult than any other method. Plasma treatment is rather expensive, very sensitive to dosage time, and labor intensive to create multiple masks.<sup>11</sup>

#### 2.2.2.3 *Channels by reshaping platform*

Fenton et al demonstrated a method for creating channels by reshaping the platform. They used an X-Y knife plotter to cut both cellulose and nitrocellulose membranes into different shapes. They examined urine for glucose, albumin, and pH using their patterned devices. A main goal of their experiment was to reduce the possibility of user error by simplifying spatial arrangement, areal arrangement, and linear layout and color coding the outside of the container for reference. Devices filled within four minutes and color fully developed after an additional 4 minutes. Fabrication by this method used no chemicals other than the detecting bioreagents.<sup>12</sup> An example of a device created by this method is shown in Figure 5 below.





Figure 5: Example of a device created by reshaping the platform. The end of each arm is cut to label the specific test that it performs.<sup>10</sup>

#### 2.2.2.4 *Wax printed channels*

Carrilho et al. developed methods for creating channels using wax. They used a commercial Xerox 8560N wax printer to print wax lines on Whatman chromatography paper. The pattern was designed in Clewin drawing software. Their patterns were printed directly onto the chromatography papers. The patterned paper was placed on a hotplate at 150C for 2 minutes.



### 1. design layout



### 2. print devices



### 3. reflow wax



Figure 6: Procedure for preparing a wax-based paper microfluidic device. 1) Design device in graphical program on computer. 2) Print design onto paper membrane substrate. 3) Heat wax to melt it and allow it to flow through the thickness of the paper<sup>9</sup>

The printer laid the wax in a channel pattern, and the hotplate heated the device to melt the wax and allow it to penetrate all the way through the paper. The wax created channels by making hydrophobic barriers within the paper. A sample will be pulled through the paper by capillary action, and bound to the channels by the hydrophobic barriers outlined by the wax. The thinnest functional hydrophobic barrier they were able to create was 850  $\mu\text{m}$  wide (300 $\mu\text{m}$  nominal width). The smallest channel width was 561  $\mu\text{m}$  wide, with a nominal width of 1100 $\mu\text{m}$ .<sup>9</sup>

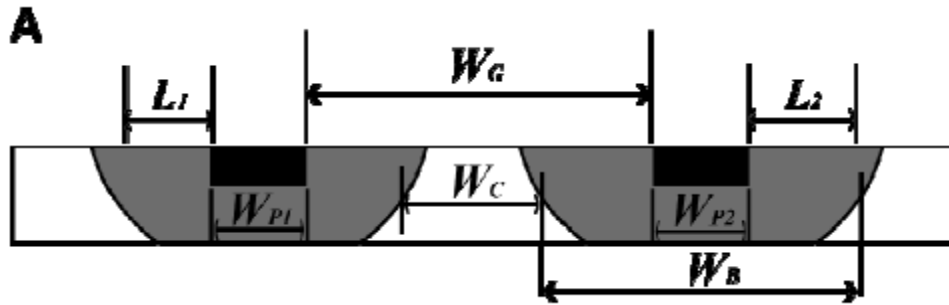


Figure 7: Channel width in Paper.  $W_g$  is the nominal width of the channel.  $W_c$  is the width of the channel after wax reflow.  $W_p$  is the width of the printed line.  $W_b$  is the width of the barrier after reflow.  $L_1$  and  $L_2$  are the horizontal spreading of the lines during wax reflow. Nominal lengths refer to the lengths in original designs<sup>9</sup>

### 2.3 Capability Gap to Be Addressed

Resources on a space shuttle are extremely limited. The astronaut has a limited amount of food aboard the ship, so will want to use as little as possible of his blood to a diagnostic chip. The desired specifications for a diagnostic device are outlined by NASA. They include: measurement time, maintenance requirements, and expandability.<sup>5</sup> It is also desirable that minimal sample procuring equipment is needed, as they tend to be one-time-use creating waste. For this reason, it is desirable to create a chip that functions solely on the sample volume obtained from a finger-stick with a lancet. The diagnostic chip should be capable of obtaining this sample directly from the finger-sticking by placing the finger on a designated collection area. The diagnostic chip should perform an entire panel using only one sample. The volume of the sample will be less than 200 uL, on which up to 7 tests will need to be performed. This allows for maximum of 28.5 uL of sample per test. California Polytechnic State University, San Luis Obispo currently does not have the ability to make devices that will work with such small samples. Manufacturing methods for minimizing sample and reagent size will have to be characterized and optimized.

### **2.3.1 Challenges to be addressed in this work**

This work will have two main goals. 1) To optimize baking settings for maximum wax penetration, and minimum lateral spreading. 2) Using the optimized baking settings, determine the smallest manufacturable functional channel widths and functional barrier widths. Manufacturing methods will have to be developed, characterized, and optimized using available equipment.

## **2.4 Summary of Intro**

There is a need for medical diagnostic tests that minimize weight, volume, and support equipment. Paper-microfluidics provides a method for making an extremely light and small diagnostic test that requires little supportive equipment. The equipment necessary to make such a test is available at Cal Poly, but manufacturing methods have not been well developed. The aim of this project is to characterize and optimize the manufacturing methods for nitrocellulose-based diagnostic chips.

## **3 Materials**

This section describes the various materials used in the present work

### **3.1 Papers**

Bibulous Paper (Hamilton Bell Co. Inc) was used for preliminary testing and refining experimental protocols. Bibulous paper is typically used in biology labs for moisture absorbance. It was used in preliminary experiments because it has similar wicking properties to nitrocellulose membrane, with a much smaller price tag. This was essential because early experiments were very high volume in order to hone in on the appropriate time and temperature ranges.

Nitrocellulose Membrane was obtained from the Hi-Flow line of EMD Millipore Corporation (Billerica, MA, USA). Three variants were used HF180, HF135, and HF75. The name of each variant represents the time (seconds) water takes to flow 4 centimeters through the substrate. The higher the model number, the slower the lateral flow.

Membrane	Capillary Flow Time Specification* (sec/4 cm)	Flow Rate	Sensitivity
HF240	240 ± 60	<div>Slowest</div> <div>↓</div> <div>Fastest</div>	<div>Most sensitive</div> <div>↓</div> <div>Least sensitive</div>
HF180	180 ± 45		
HF135	135 ± 34		
HF120	120 ± 30		
HF090	90 ± 23		
HF075	75 ± 19		

\*The range is for all measured values on a roll and represents  $\pm 3 \sigma$ ; the acceptable range for the mean is  $\pm 10\%$  of the target.

**Table 1: Millipore Corp's selection of Nitrocellulose Membrane<sup>1</sup>**

## 3.2 Lab Equipment

### 3.2.1 XEROX ColorQube 8570



**Figure 8: Xerox 8570N. Capable of printing 2400l using wax ink<sup>2</sup>**

The printer used was a ColorQube™ 8570 by XEROX Corporation, with Xerox ColorQube Wax Ink, also from XEROX Corporation. It prints using colored wax rather than traditional laser toner or liquid ink. The wax blocks are loaded into the ink bay at the top of the printer. Spring loaded plates then press the blocks down into the heated ejection heads when the lid is closed. When first powered on, the printer goes through a warm-up phase during which melts some “start-up” wax in the melting chamber. During printing, it dispenses the melted wax onto the media and melts more wax to replenish the stock. The manufacturer claims 2400DPI to be the maximum effective resolution.



Figure 9: Loading Ink to XEROX 8570N. The wax blocks are loaded manually into the ink bay of the 8570.<sup>3</sup>

### 3.2.2 Food Coloring (FD&C Blue No. 1)

Deionized water was used for all mixtures during functional testing. For flow and barrier functionality testing, blue food coloring (disodium salt of ethyl [4-[*p*-[ethyl (*m*-sulfobenzyl) amino]- $\alpha$ -(*o*-sulfophenyl) benzylidene] - 2,5 -cyclohexadien - 1 - ylidene] (*m*-sulfobenzyl) ammonium hydroxide)<sup>4</sup> was added in a 1:30 ratio (blue food coloring to water) to improve visualization of fluid flow.

### 3.2.3 Lab Oven

Samples were baked in an ED23 gravity convection heating oven by Binder GmBh (Tuttlingen, Germany).

### 3.2.4 Additional Equipment

An Olympus microscope was used to capture images. The ratio of image pixels to millimeters was determined using a calibrated scale. The microscope used was an Olympus.

SEM images were taken on a TM-1000 tabletop environmental SEM (Hitachi Ltd. [Tokyo, Japan](#))

Micropipettes by Fisher Scientific were used to apply sample solution to test devices.

## 3.3 Software

Inkscape is a cross-platform open source vector graphics editor. The Windows version of Inkscape 0.48 was used to design and print all devices in this project

ImageJ is a public domain image analysis program developed by the NIH. ImageJ was used in image analysis.

## 4 Methods and Results

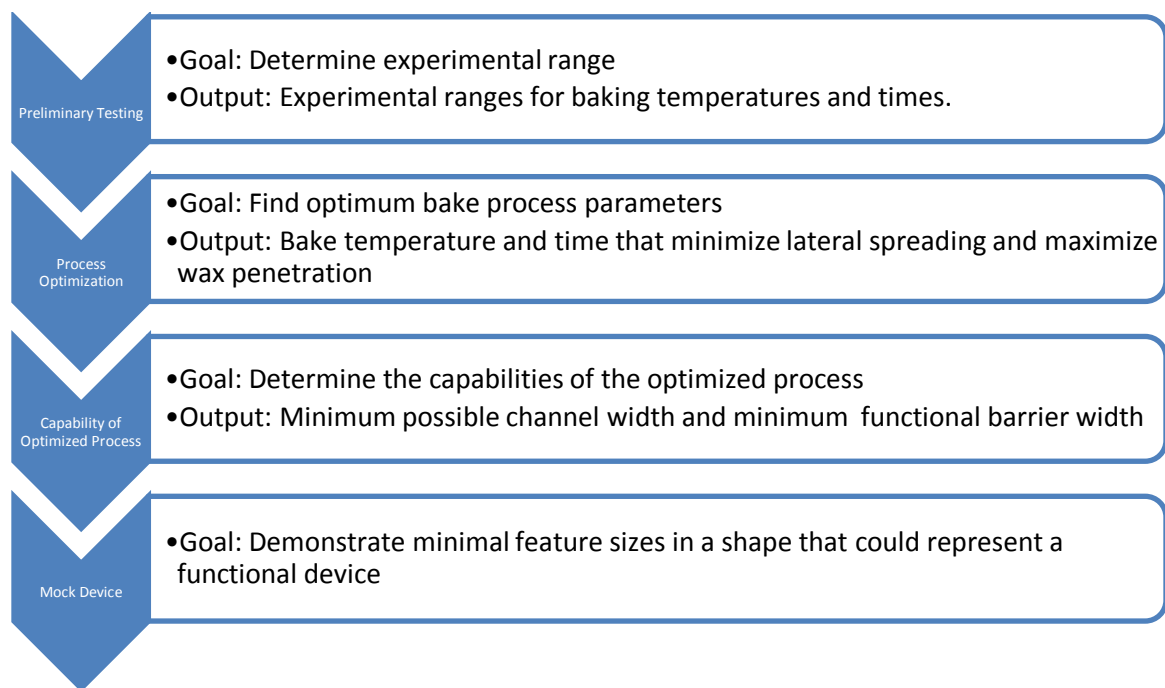


Figure 10: Summary of Methods and Results

### 4.1 Determining Optimal Baking Times and Temperatures

To determine the optimal baking temperatures, first, preliminary testing was performed using bibulous paper to determine the appropriate ranges of interest for bake temperature and time. The time and temperature ranges were then varied to determine the optimum combination (full depth wax penetration, while minimizing lateral spreading,) in three different models of NC membrane.

### 4.2 Determining Experimental Range

Preliminary testing was performed to determine appropriate experimental ranges for temperature, time, and feature widths. Preliminary testing was performed using bibulous paper, due to its lower cost and easier handling compared to nitrocellulose membrane. Small boxes were drawn in InkScape, then printed onto bibulous paper using the wax printer. These samples were baked at various times and

temperatures, and then inspected for visible penetration of the wax into and through the paper. These observations were used to determine the valid temperature and time ranges for use in nitrocellulose membrane, and are listed in Table 2: Experimental Ranges for Time and Temperature.

Temperature (Degrees Celsius)		Time (seconds)
95C		0
110C		5
125C		10
150C		15
		25
		35
		45
		60

Table 2: Experimental Ranges for Time and Temperature. All combinations of temperature and bake time were evaluated

## 4.3 Process Characterization and Optimization

The process was characterized to determine the dependence of wax reflow on time, temperature, paper type. This knowledge was then applied to determine the minimum feature sizes possible, and then demonstrated in a mock device.

### 4.3.1 Wax Reflow Characterization

To characterize this process, the following protocol was followed:

1. Using Inkscape, draw 0.5mm wide lines:





Figure 11: Group of 0.5mm wide lines. These lines were used to characterize the process at various parameters

2. Print sample by sending InkScape drawing to Xerox 8570N
  - a. Black Ink used
  - b. Settings: Maximum resolution, Picture Quality
3. Preheat oven to desired temperature. After oven display reads desired temperature, Allow at least 5 minutes for temperature to stabilize
4. Place sample on aluminum foil 'tray'
5. Quickly, open oven door and place tray into oven, and reclose the door and start timer for appropriate time
6. Open oven door and remove sample when timer runs out
7. Cross-section sample using a razor blade to cut perpendicular to the line
8. Image cross-section of sample using microscope

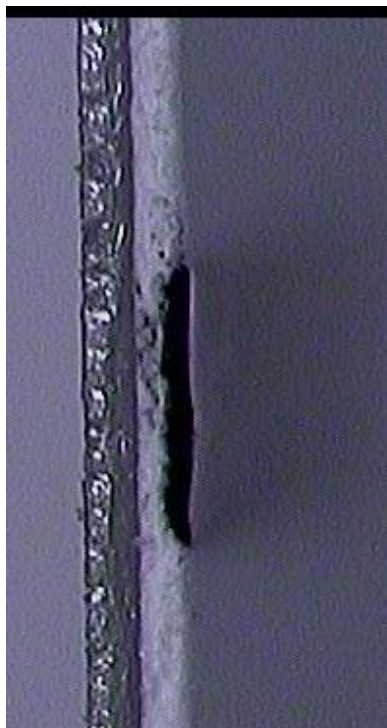


Figure 12: Example of cross-section. HF180, 125C, 10 Seconds

9. Determine distance of wax lateral spreading and penetration using ImageJ
  - a. Wax was considered fully penetrated when the deepest portion reached the polymer backing and was essentially as wide as the shallowest point.

#### 4.3.1.1 *Results*

As time increased, wax penetration and spreading increased.

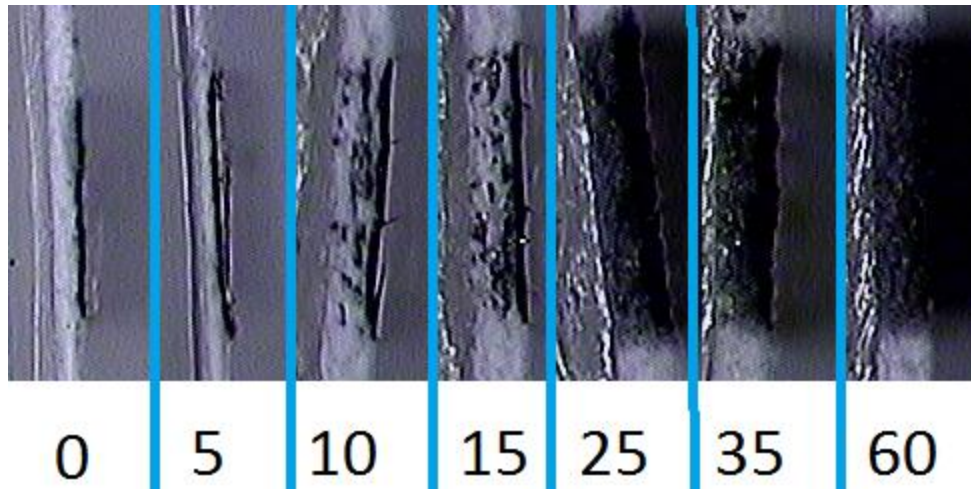


Figure 13: Cross-section of Wax Flow Over Time. Time (seconds) on X-axis. HF180 membrane, 95°C. Full penetration is only present in the 60 second sample, as the 35 and 25 second samples have some visibly white nitrocellulose membrane near the clear plastic backing. The line gets visually wider as bake time increases.

Membrane: HF75					Membrane: HF135				Membrane: HF180						
Time (seconds)		Temp. Celsius					Temp. Celsius					Temp. Celsius			
		90	110	125	150		90	110	125	150		90	110	125	150
	0														
	5														
	10				1.60					1.20					
	15			1.55	1.71		1.11	1.33	1.27		1.15	1.20	1.16		
	25		1.50	1.58	1.76		1.31	1.36	1.33		1.19	1.25	1.24		
	35		1.50	1.67	1.85		1.37	1.42	1.46		1.22	1.25	1.27		
	45	NA	1.59	1.83	1.94	NA	1.40	1.48	1.51	NA	1.26	1.30	1.32		
	60	1.44	1.80	1.87	1.99	1.29	1.47	1.40	1.56	1.22	1.33	1.36	1.37		

Table 3: Wax spreading as a function of Temperature, Time, and Membrane model. Red indicates that full thickness penetration did not occur for any samples. Orange indicates that some samples had full thickness penetration, but 1 or more samples had incomplete penetration. Green indicates that all samples had full-thickness. The number on the green rectangles is the spreading ratio (ratio of the average line width compared to the desired line width)

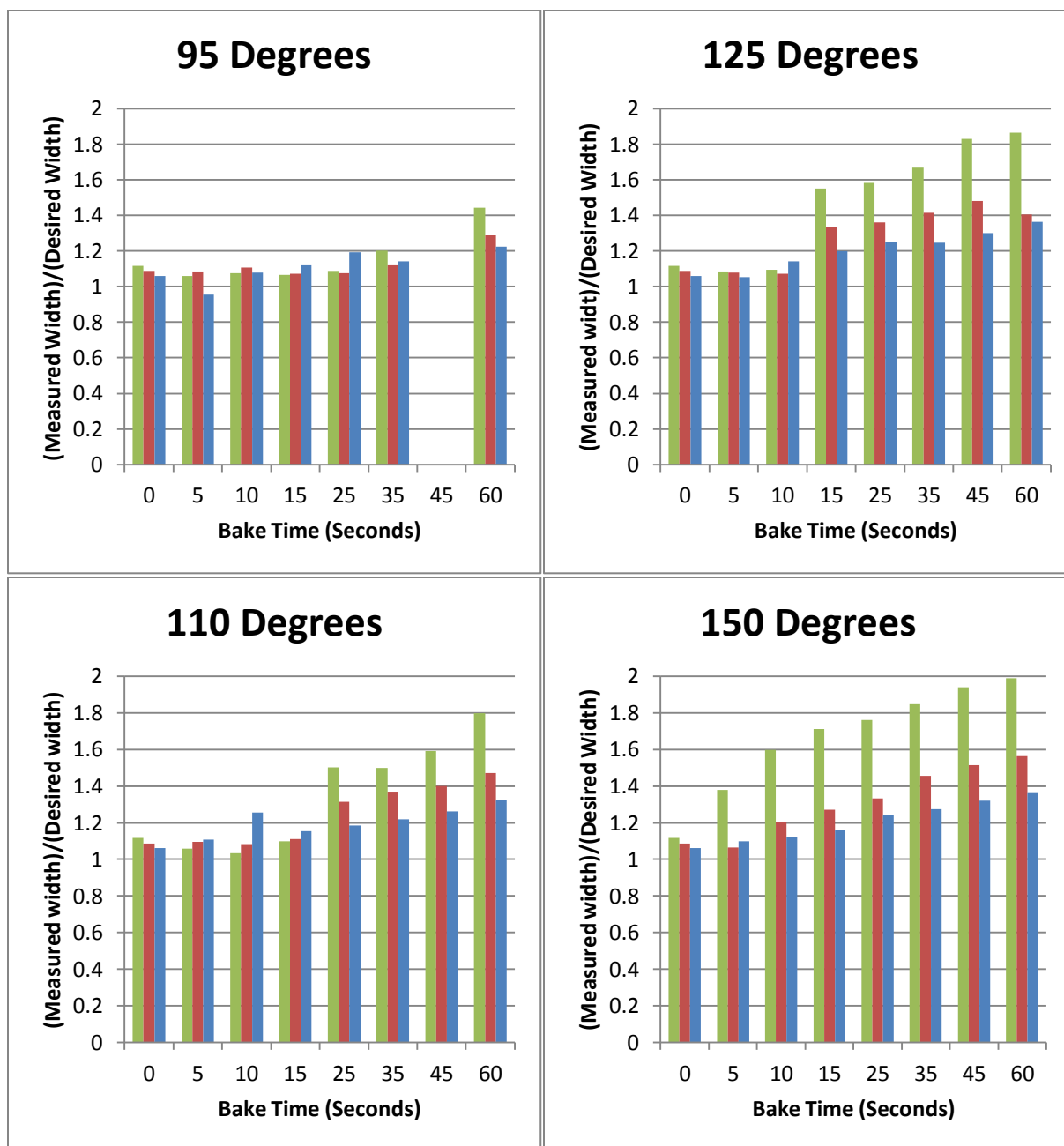


Figure 4: Lateral Spreading, as a ratio of Desired Printed Width. Line width increased with increased bake time and/or temperature. Higher speed lateral flow paper models had consistently higher spread ratio. Note: 45 seconds at 95°C was accidentally skipped during device preparation

Key:

- HF75
- HF135
- HF180

#### 4.3.1.2 Discussion

It is clear that wax spreading increases with time, temperature, and membrane flow rate. HF75 had significantly higher spread than the other two models. This is expected, because HF75 has the fastest flow rate of all three models.

The best spreading ratio that also achieved full penetration was 15 seconds at 110°C using HF135. This combination resulted in a line that fully penetrated the thickness of the paper and only spread to 1.11 times its intended size. For further testing, 90°C for 60 seconds was the recipe chosen because it is only marginally more spreading than 1.11, was the easiest to control, (the long time spent in the oven reduces variability due to slight changes in oven placement and removal) and it had low variation in spreading ratio between membrane models.

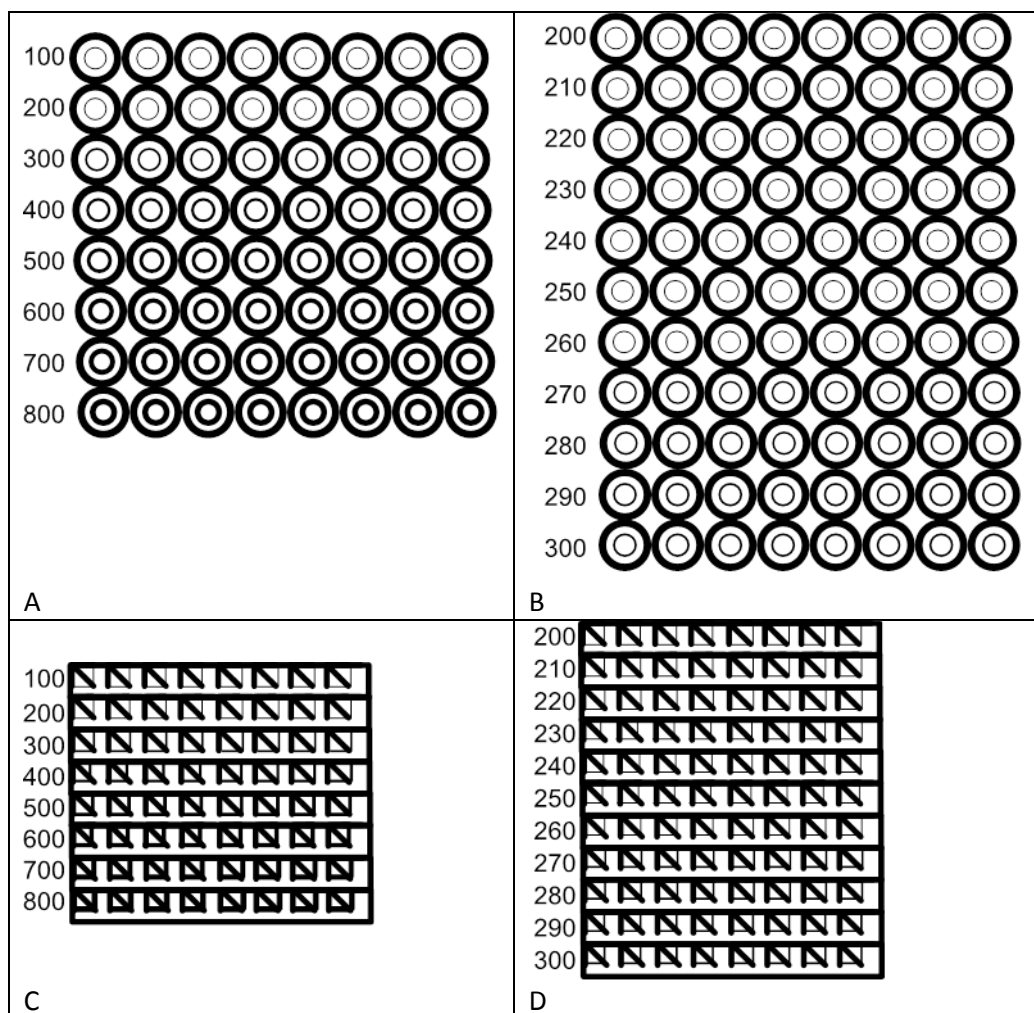
### 4.4 Practical Application – Minimal Feature Sizes

The knowledge of the baking process developed in section 3.3, was used to minimize the functional feature sizes of barriers and channels; the two main features of a paper microfluidic device.

#### 4.4.1 Determination of minimum functional barrier width

Devices were designed to test line widths capable of creating a functional fluid barrier. A functional barrier was defined as a line that would prevent the movement of water for at least 5 minutes. Circular (Pattern A and B), straight lines (Pattern C and D) were tested. The circular patterns have a center circle, with the indicated line width listed in microns to the left. The test liquid was placed into the center of the inner circle, and would be considered a failure if the liquid leaked out within 5 minutes. To fit a large number of tests onto a small amount of paper, the test circles are separated by thick (800µm) circles. Similar design methodology was used for the straight line testing (patterns C and D). The straight line devices have horizontal and vertical lines in a row, with one large reservoir for each wall thickness. The reservoir was filled with testing fluid, and allowed to sit for five minutes. If the fluid

leaked into the white triangle behind the test barrier, that barrier was considered a failure. Preliminary testing showed that 200 $\mu$ m barriers would likely fail, and 300  $\mu$ m barriers would likely pass, so patterns B and D were designed to further characterize that window. Patterns A-D shown in Figure 14 below were printed simultaneously baked at 95C for 60 seconds. HF135 was used as the representative model due to the limited availability of the other membrane models. Barrier widths are listed as the nominal (designed) widths, in microns.



**Figure 14: Design of Devices to Test Minimal Functional Barrier Width. A and B are designed to test circular barriers. C and D are designed to test vertical and horizontal straight line barriers.**

These patterns were printed onto all three models of nitrocellulose membrane and baked at 95 degrees for 60 seconds. This recipe was chosen because it was the best overall for all paper models.

#### 4.4.1.1 Results

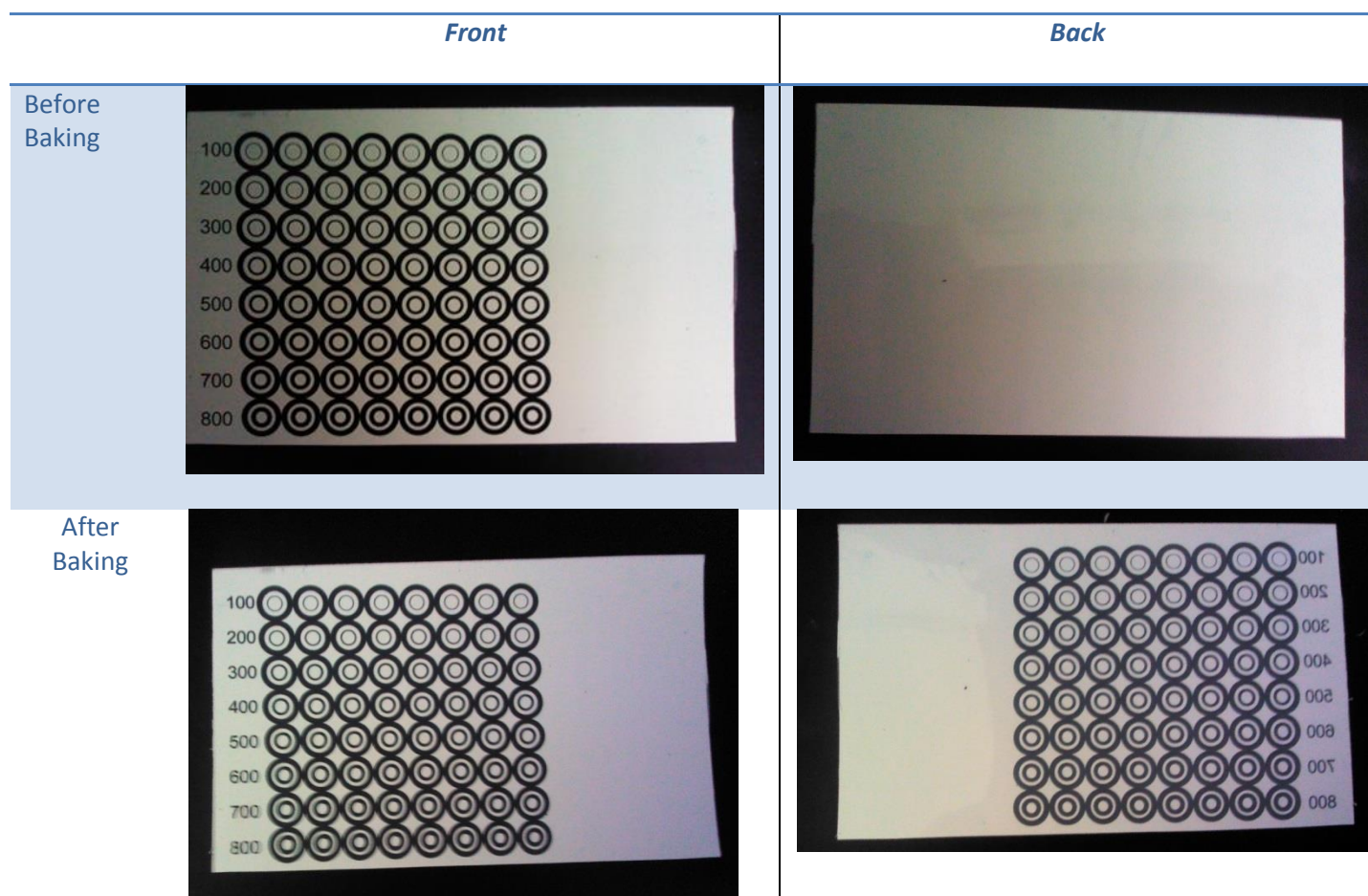


Figure 15: Images of Barrier Width Device before and after printing. Before baking, the back is completely white. After baking, the pattern can be seen melted through the membrane.



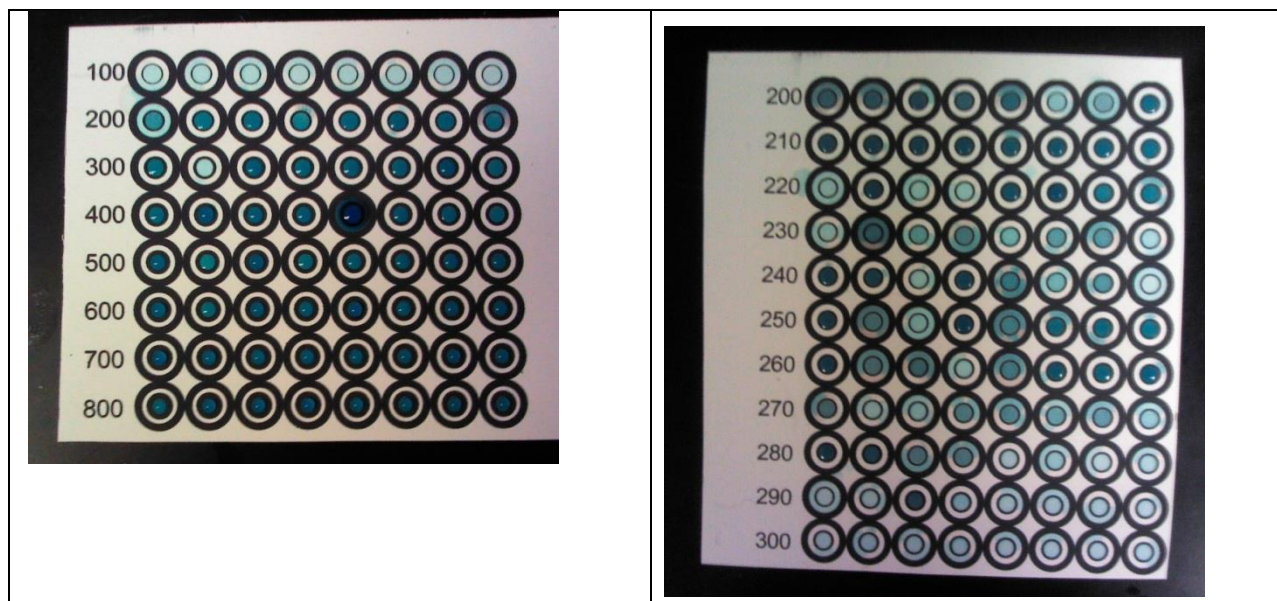


Figure 16: Round Barrier Width Devices 5 minutes after applying solution: 100 to 800um range (Left) (note: 5th circle in row 400 looks like a failure but was due to a pipetting error.) 200 to 300 um range. (Right)

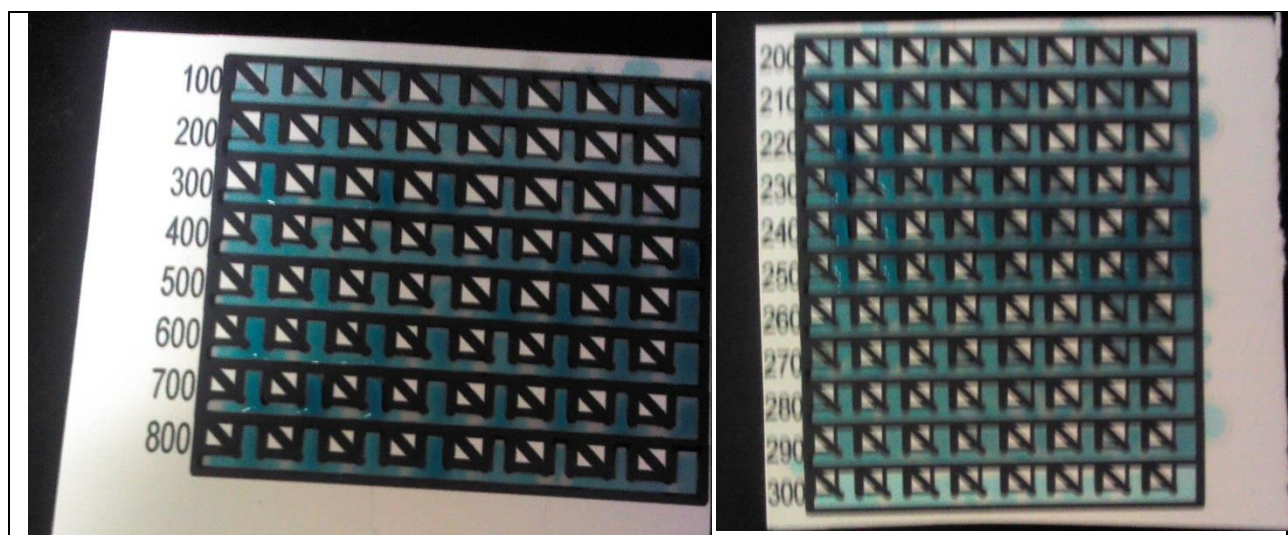


Figure 17: Straight Line Barrier Width Devices 5 minutes after apply solution. 100 to 800um range (Left). 200 to 300um range (Right).

#### 4.4.1.2 Discussion

After baking at 95°C for 60 seconds, a 400 um wide line will create a hydrophobic barrier. 300 um lines were sometimes sufficient to create a barrier, but occasionally had leakage. This was true for circles, horizontal lines, and vertical lines. It was seen that at some intersections of the non-experimental lines,



there was some fluid leakage. It is not apparent why this leakage can occur, since the intersecting lines are thicker than 400um.

#### 4.4.2 Determination of minimum functional channel width

Devices were designed to test the width necessary to produce a functional channel.

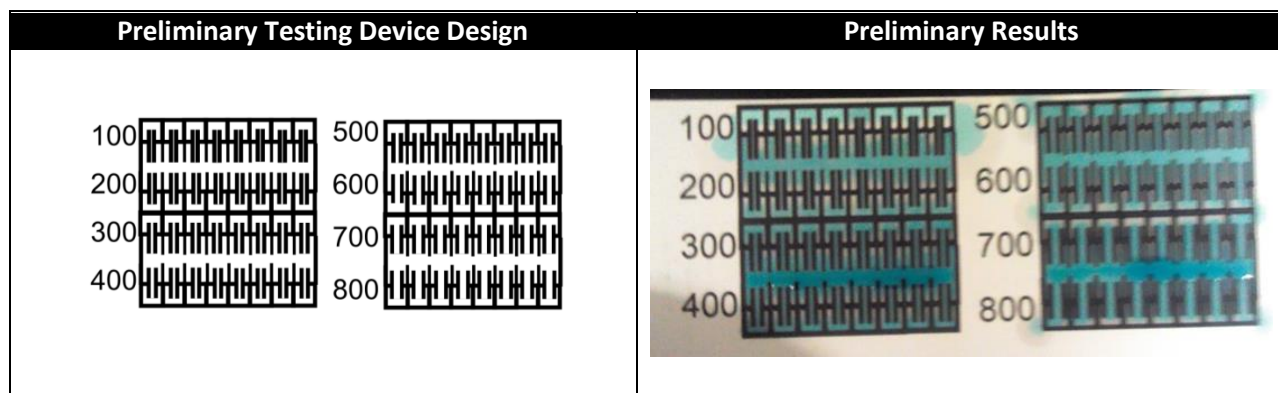


Figure 18: Preliminary Channel Width Testing. Leakage at the corners is unexpected and remains unexplained.

Preliminary testing showed the minimum channel width would definitely be less than 400um, and probably less than 200um. To determine the minimum channel width, devices were designed with 100-400um and 100-175um ranges, and printed on all three models of nitrocellulose paper, then baked at 95°C for 60 seconds.

#### 4.4.2.1 Results

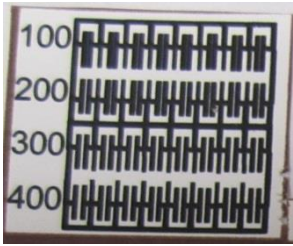
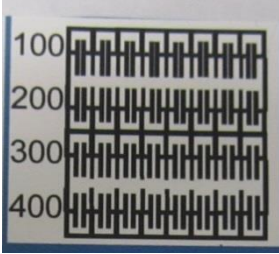
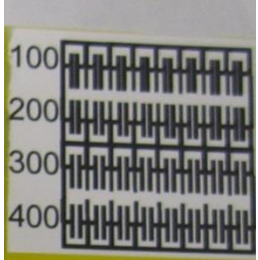
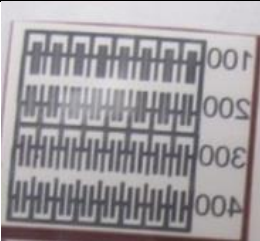
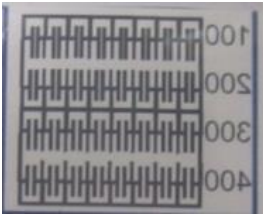
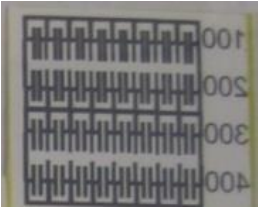
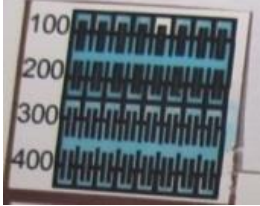
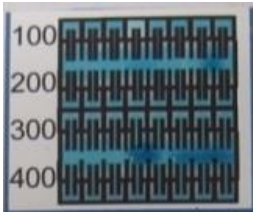
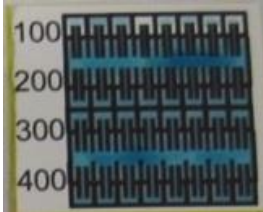
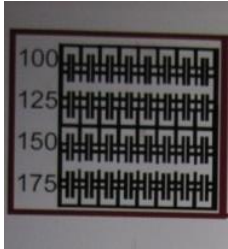
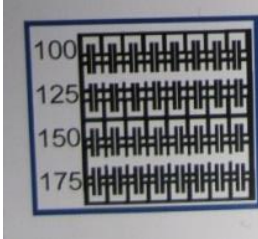

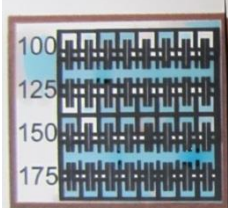
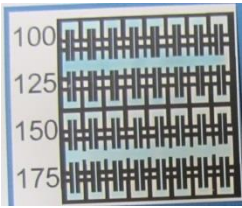
	HF75 Membrane	HF135 Membrane	HF180 Membrane
<b>Devices After Baking</b> <i>100-400 <math>\mu</math>m Range</i> <i>Front View</i>			
<b>Devices After Baking</b> <i>100-400 <math>\mu</math>m Range</i> <i>Back View</i>			
<b>Devices after fluid flow</b> <i>100-400 <math>\mu</math>m Range</i> <i>Front View</i>			
<b>Devices After Baking</b> <i>100-175 <math>\mu</math>m Range</i> <i>Front View</i>			
<b>Devices After Fluid Flow</b> <i>100-175 <math>\mu</math>m Range</i> <i>Front View</i>			Missing

Figure 19: Channel Width Testing Devices Results

#### 4.4.2.2 Discussion

After baking at 95°C for 60 seconds, a channel designed 175  $\mu\text{m}$  wide will allow fluid to flow in any paper model. The minimum functional channel size was 100 $\mu\text{m}$ , but was only reliable when using HF135 membrane. This result is expected because comparatively higher wax lateral flow in HF75 will cause the channel to narrow more than in HF135. Note: the results image of the range 100-175 $\mu\text{m}$  channel device made on HF180 membrane was lost, so results for that model are unknown. It is believed that the results are similar to those of the other two membranes because it was found to have a similar lateral flow rate in characterization testing (see section 4.3.1.1).

#### 4.4.3 Mock Devices

To test the ability of 150  $\mu\text{m}$  channels in when printed in multiple directions, mock devices were designed. These mock devices are also a possible model for doing multiple single-reaction tests (one at the end of each spoke of the 'wheel') with a single sample placed in the center.

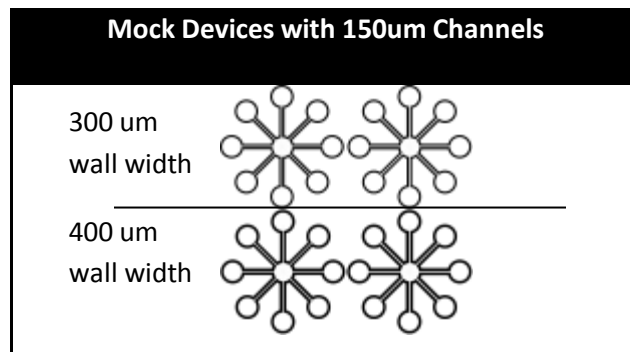


Figure 20: Design of Mock Devices

#### 4.4.3.1 Results


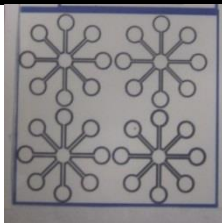
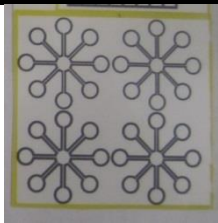

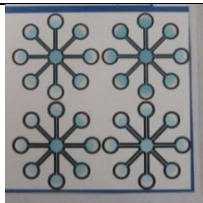
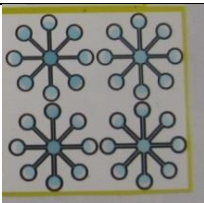
	HF75 Membrane	HF135 Membrane	HF180 Membrane
<b>Mock Device</b> <i>After printing and baking at 95°C for 60 sec</i>			
<b>Mock Device</b> <i>After Fluid Flow</i>			

Figure 21: Results of Mock Device Testing

#### 4.4.3.2 Discussion

Fluid successfully flowed through 150um channels from the center circle to the outer circles on the HF135 and HF180 membrane mock devices. Only some of the channels printed on HF75 membrane were shown to be functional. This agrees with the results in the channel width testing, which showed that a 150um channel would not be blocked in HF135, but might be occasionally blocked in HF75(section 2.2.3.3). None of the mock devices showed any leakage with either 300um or 400um barriers.

## 5 Conclusion

### 5.1 Optimal Process Parameters

To create a device with minimal feature sizes devices should be printed onto HF135 membrane, and then baked at 110°C for 15 seconds. However, these settings may be more susceptible to variation

in the time it takes to place/remove them into/out of the oven. Also, if the device must be made on multiple types of membrane, 95° for 60 seconds produced the optimal overall results for all models.

This process could be further improved by better regulating the amount of time the devices are baked, and increasing temperature uniformity in the oven. One way this could be accomplished is with a conveyor style oven.

## **5.2 Minimal Functional Feature Size**

### **5.2.1 Functional Barrier Width**

In this work, we were able to demonstrate that when baked for 60 seconds at 95°C, a 400um line will create a functional barrier in circular, horizontal, and vertical orientations. This barrier width was demonstrated in a mock multiplex single-reaction test device.

### **5.2.2 Functional Channel Width**

In this work, functional channels were created by baking devices at 95°C for 60 seconds. The minimum reliable channel size was 100um using HF135 membrane. The smallest reliable channel size across all membrane models was 175um. A 150um channel was demonstrated to be functional in a mock multiplex single-reaction test device printed on HF135 and HF180 membranes.

### **5.2.3 Future Work**

Using the recipe in this work, a device can be quickly designed and prototyped to get the proper fluid flows for a functional test. However, to develop a useful test, it will be necessary to determine ways to perform critical chemical reactions within a paper substrate, and compare those results to industry standards.

The work in this project could be refined to further minimize the device size. The barrier width region between 300um and 400um was not explored in this work. It is possible that additional

experimentation would show a minimal barrier width within that range without modifying any process parameters.

The corner leakage issue (such as in the bottom left image in Figure 19: Channel Width Testing Devices Results) is concerning, since the leaking lines are considerably wider than other lines that have shown to create functional barriers. This issue seemed to only occur at right-angle intersections between two thick lines, but it is unknown if this is the cause. It is possible that due to the high concentration of wax at these areas, not enough heat was able to dissipate in to melt all the wax in the center of the area. With further fine-tuning, a smaller (300um) line could likely create a functional barrier as this width only showed occasional leakage. Factors that could be assessed to improve these issues are orientation in the oven, air convection, or as above, this could be accomplished with a conveyor belt style oven.

## 6 Works Cited

1. Lab on paper. *Lab Chip* **8**, (2008).
2. Hay Burgess, D. C., Wasserman, J. & Dahl, C. A. Global health diagnostics. *Nature* (2006).
3. Barbara Lujan & White, R. Human Physiology in Space. at  
<<http://www.nsbri.org/humanphysspace/index.html>>
4. Stevens, L. A., Coresh, J., Greene, T. & Levey, A. S. Assessing Kidney Function — Measured and Estimated Glomerular Filtration Rate. *New England Journal of Medicine* **354**, 2473–2483 (2006).
5. Space Medicine Division Exploration Medical Capability Functional Requirements Document. (2011).
6. Walt, D. R. Miniature analytical methods for medical diagnostics. *Science* **308**, 217+ (2005).
7. Martinez, A. W., Phillips, S. T., Butte, M. J. & Whitesides, G. M. Patterned Paper as a Platform for Inexpensive, Low-Volume, Portable Bioassays. *Angewandte Chemie International Edition* **46**, 1318–1320 (2007).
8. Andres W Martinez, Scott T. Phillips & George M. Whitesides Diagnostics for the Developing World: Microfluidic Paper-Based Analytical Devices. *Analytical Chemistry* **82**, 3–10 (2010).
9. Carrilho, E., Martinez, A. W. & Whitesides, G. M. Understanding Wax Printing: A Simple Micropatterning Process for Paper-Based Microfluidics. *Anal. Chem.* **81**, 7091–7095 (2009).
10. Lu, Y., Shi, W., Qin, J. & Lin, B. Fabrication and Characterization of Paper-Based Microfluidics Prepared in Nitrocellulose Membrane By Wax Printing. *Anal. Chem.* **82**, 329–335 (2009).
11. Li, X., Tian, J., Nguyen, T. & Shen, W. Paper-Based Microfluidic Devices by Plasma Treatment. *Anal. Chem.* **80**, 9131–9134 (2008).
12. Fenton, E. M., Mascarenas, M. R., López, G. P. & Sibbett, S. S. Multiplex Lateral-Flow Test Strips Fabricated by Two-Dimensional Shaping. *ACS Appl. Mater. Interfaces* **1**, 124–129 (2008).
13. Szűcs, J. & Gyurcsányi, R. E. Towards Protein Assays on Paper Platforms with Potentiometric Detection. *Electroanalysis* **24**, 146–152 (2012).

14. Dungchai, W., Chailapakul, O. & Henry, C. S. Use of multiple colorimetric indicators for paper-based microfluidic devices. *Analytica Chimica Acta* **674**, 227–233 (2010).
15. Yu, J., Wang, S., Ge, L. & Ge, S. A novel chemiluminescence paper microfluidic biosensor based on enzymatic reaction for uric acid determination. *Biosensors and Bioelectronics* **26**, 3284–3289 (2011).